

Characterization of Single Pixel Evaluation PIV for Precise Flow Measurement

Han-Sheng Chuang¹, Steve T. Wereley¹, Lichuan Gui²

1: School of Mechanical Engineering, Purdue University, West Lafayette, IN, U.S.A., swereley@purdue.edu

2: National Center for Physical Acoustics, University of Mississippi, MI, U.S.A., lcgui@olemiss.edu

Abstract Single pixel evaluation (SPE) is used to increase the resolution of PIV to its physical limit of one pixel. This novel approach is simple, intuitive and compatible with current PIV hardware and software. Theoretically, to reach the same signal-to-noise ratio (SNR) in conventional spatial cross-correlation with a 32×32 pixel interrogation window, 1024 image pairs are required in SPE. However, this simple scaling relation does not hold in every instance. To clarify the reasons why it does not, this article investigated four major factors determining SPE performance. These include image quality, particle density, search radius, and particle image size. SPE performance is quantified using three measures: random error, total error, and correlation coefficient. Simulated particle images subjected to parabolic flow were used throughout this study. The results indicate that to a large extent image quality determines the quality of the SPE results. When using small image sets (≤ 1024 image pairs), a SNR of at least 12.39 dB is strongly recommended. Particle density is another important factor that should be carefully controlled. Neither dense nor sparse concentration was acceptable but rather a moderate concentration. In this case, since the displacement was not large (\leq five pixels), a specific concentration, 80 particles over 64×64 pixels, was found to perform better than all other concentrations. Larger search radius and smaller particle image size were also found to increase the accuracy of the SPE technique. SPE was also compared with an equivalent cross-correlation algorithm. Without background noise, the results of SPE showed good agreement with the actual flow and had small random error. However, when background noise was considered, performance degraded considerably. We characterized the intrinsic SPE performance by varying controlled factors. The behaviors in SPE were thoroughly investigated and discussed via the simulated particle images. Eventually, specific parameters were suggested for the general SPE applications in the end of the text. Further experimental measurements will be employed to verify the findings in the near future.

1. Introduction

Single pixel evaluation (SPE) is a robust algorithm useful for increasing the spatial resolution of μ PIV from microscale to nanoscale (*Westerweel et al., 2004*). The key idea is to replace the spatial correlation average with a temporal one—commonly used in μ PIV—averaged over just a single pixel. Thus, in situations where it is possible to acquire thousands of image sets in the region of interest, one can shrink the interrogation window size from thousands of pixels (e.g. 32×32 pixels) to a single pixel while maintaining the same signal-to-noise ratio (SNR) as in conventional spatial cross-correlation. Some studies have already demonstrated that this technique works using both actual and simulated flows (*Westerweel et al., 2004; Wereley et al., 2005; Sud, 2005*). However, the reliability and accuracy of the SPE algorithm have not yet been examined closely. Discrepancies have been observed between analytical results and SPE results, indicating that further study is needed.

Depending on the past works on improving conventional cross-correlation, several factors such as particle diameter, interrogation window, and the like were usually considered. *Fincham et al. (1997)* showed the errors got worse as the interrogation window size shrank. Moreover, an optimal range of particle image size for a certain interrogation region was also observed. *Prasad et al. (1992)* and *Westerweel et al. (1997)* further indicated two to three pixels would result in least variance. Particle image size, and particle density were studied by *Huang et al. (1997)* in order to quantify and reduce the error of digital PIV. It showed that low particle image density tended to cause large

mean bias error, and modest particle image size could reduce the error. Typically, the measurement errors are decomposed into two forms; namely the bias error and random error. Their influences on PIV and corresponding improved methods have been well discussed by a number of papers (*Fincham et al., 1997; Gui et al., 2002; Huang et al., 1997; Wereley et al., 2005*).

In the following, a series of simulated particle images with a parabolic flow profile were generated from a custom-written PIV package called EDPIV (http://eo.yifan.net/users/lcgui/Edpiv_intro.htm). Based on the previous works, four factors, namely particle image quality, particle density, particle image size and search radius (SR), were investigated in this article. All of them were evaluated by measurement errors and their correlation coefficients with the actual flow profile. The results suggested an ideal SPE computation, i.e. accurate and reliable, may need the following conditions: (i) a certain particle image density, 80 particles over 64×64 pixels in this case; (ii) small particle image size; (iii) large search radius, i.e. sufficient to cover the required spatial information; and (iv) high image quality. The image quality was the most significant of these factors. Compared with the fast Fourier transform cross-correlation (FFT-CC) under the same SNR, the results from SPE performed better without background noise but worse with background noise. It implied more image pairs would be needed in practice when an equivalent SNR was expected. Eventually, the analyses were contributed to general criteria for further SPE applications.

2. Methods

2.1 Algorithm of Single Pixel Evaluation (SPE)

As shown in Figure 1a, the operation of conventional spatially-averaged cross-correlation typically needs two multi-pixel interrogation windows to calculate one valid displacement vector. Ideally, the second window contains all of the information from the first one and no velocity gradient occurs inside the region. Under these conditions a perfect correlation peak indicating the true in-plane displacement will be obtained. The mathematical expression for such a spatially-averaged correlation is written as

$$\Phi_{cc}(m, n) = \sum_{x=1}^P \sum_{y=1}^Q f(x, y) \cdot g(x + m, y + n), \quad (1)$$

where P and Q denote the side lengths in pixels of the interrogation window in x and y direction, respectively. f and g are the intensity functions of the first and the second windows. m and n are the displacement in the correlation domain. The parameters that may influence the accuracy perhaps come from the particle density, image quality, and interrogation window size. Obviously, enlarging the window size is a way to ensure that sufficient spatial information is included. However, large interrogation regions may result in serious bias errors when a strong velocity gradient is present in the flow as well as a reduction in spatial resolution. To solve this problem, a novel algorithm named single pixel evaluation (SPE) was proposed (*Westerweel et al., 1997*) to drastically increase the spatial resolution without decreasing SNR. The cross-correlation function from Equation (1) can be rewritten for an interrogation region consisting of a single pixel averaged over k different time steps can be expressed as follows

$$\Phi_{spe}(m, n) = \sum_{k=1}^N f_k(x, y) \cdot g_k(x + m, y + n), \quad (2)$$

where N is the number of image pairs (*Gui et al., 2002*). As illustrated in Figure 1b, the main concept is shrinking the interrogation window to its physical limitation given the pixilated format in which the images are recorded: one pixel and collecting the spatial information by searching the second pixel within some specified radius. Based on the ensemble correlation average (*Meinhart et al., 2000*), the SNR can be increased by increasing the number of image pairs in a given sample.

For instance, if a particle density with 10 particles over a 32×32 pixel window (9.77×10^{-3} particle/pixel) is used in conventional cross-correlation, at least 1024 image pairs will be needed in SPE in order to reach the same SNR, i.e. particles per pixel.

2.2 Image Simulation

For characterization of SPE, a series of well-controlled simulated particle images were generated by EDPIV varying the several factors discussed above. All the image sizes were 64×64 pixels. Except for the search radius, the rest of the factors are depicted in Figure 2, which helps the reader to visualize the relationship among these factors. The first row demonstrates the image quality. It is quantified by signal-to-noise ratio. Here 1.34 dB stands for the poorest image quality, in which the particles are hardly distinguished from the background noise while 47.96 dB stands for the best quality without any interferences. The second row demonstrates five different particle densities from the sparse 20 particles to the dense 200 particles. Since the sparse case lowers the SNR and the dense one deteriorates the determination of displacement, an optimal number can be expected. The last row demonstrates the particle image sizes from one pixel to six pixels. Despite the extreme case (one pixel) never takes place in reality due to the diffraction limit, a theoretical simulation is still believed contributing to the understanding of SPE.

In this article, the parabolic curve (Figure 3) was preferred to govern the flow behavior throughout the entire study since many channel flows are driven by the pressure gradients and bias errors derive from the second derivative of the velocity field. The velocity profile equation is written as

$$D_i = D_{\max} \left[1 - \left(\frac{y_i}{R} \right)^2 \right], \quad (3)$$

where R is half of Y , y_i is the lateral position across the flow, and D_{\max} is the maximum displacement of the flow, which is set at five pixels.

In Figure 3, the actual calculated area (red dash square) is always smaller than the whole image size due to the search radius (SR). That is, the small strips of boundaries will not be interrogated in this study. Typically, small search radius helps the computation to approach the boundary. However, the determination of search radius has to depend on the maximum displacement of the flow.

2.3 Measurement Error Analysis

Regarding the measurement errors in PIV, two common forms are usually discussed, namely random error (σ) and the bias error (β) as expressed in Eq. (4) (Gui et al., 2002).

$$\delta = \sqrt{\frac{1}{N} \sum_{i=1}^N (x_i - x_0)^2} = \sqrt{\beta^2 + \sigma^2}, \quad (4)$$

where x_i is the individual displacement along the row, and x_0 is the actual value obtained from the simulated particle images directly. Basically, they indicate how the quality of the result is and how much effort we might put on to improve the result. The first term (σ) could be resulted from various noises, human operation and some unknown uncertainties. Since it is random, no direction-oriented, one can simply eliminate it by using a large number of data. Here the random error level is usually quantified with the root-mean-square (RMS)

$$\sigma = \sqrt{\frac{1}{N} \sum_{i=1}^N (x_i - \bar{x})^2}, \quad (5)$$

where \bar{x} is the average value of all data in same row, and N is the number of calculated data. Therefore, a displacement vector map may be resulted from an ensemble average over 1024 or 8192 image pairs and then the random errors will be obtained from each row of the data across the flow

profile. The second term (β) is caused by more complicated reasons, which had been quantitatively discussed by previous researchers (*Westerweel et al., 1997; Huang et al., 1997; Chen et al., 2005*). It is usually a periodic vibration unable to be removed by the previous way. Since this term is always coupled with the random error, It will be convenient to show the total error instead of either one in this article. Thus, as the number of data is large enough, the total error will be almost identical to the bias error because the random error is suppressed spontaneously; otherwise it will only show the composite effect.

3. Results and Discussion

The results of SPE with respect to different factors were investigated from different perspectives in the following text. Two image bases, 1024 image pairs and 8192 image pairs, were considered. Basically, the examined indices include the measurement errors and correlation coefficients. The former had been explained in the previous section; the latter would be used to indicate the agreement between the data and the actual flow profile.

3.1 Image Quality

Five image qualities ranging from 1.34 dB to 47.96 dB were compared with each other. Noted that the image quality was also quantified by signal-to-noise-ratio but using different definition and unit. To distinguish from the previous one, it was labeled as “image SNR”. As shown in Figure 4a, only does the image SNR over 12.78 dB show good agreement with the actual flow profile when a 1024 image base was considered. Similarly, serious fluctuations of total error are shown in Figure 5a as the image SNR is below 12.78 dB. However, the situation is drastically improved after the number of image is increased to 8192 as shown in Figure 6a, implying the SNR is compensated by the influx of large number of image. Despite the poor SNR seems able to be overcome by simply increasing the image, it is always a good strategy to maintain the image SNR above some specific level in case unexpected noises adulterated with the useful data. Especially, for some real cases, increasing the number doesn't always work out because the image structure could be interfered with more complicated noises. Therefore, advanced image processing such as spatial filter could be a good way to raise the image SNR. Figure 7 reveals an attempt to remove the noise by applying a threshold. The result shows a great improvement in Figure 7b, which corrects the most spurious vectors in Figure 7a after the image SNR is increased.

3.2 Particle Density

As mentioned previously, both sparse and dense concentrations could cause difficulties in resolving the displacement. Hence, a certain number of density is anticipated in SPE computation. In this case, 20 to 200 particles over 64×64 pixel image with slight background noises were evaluated. In Figure 6b, the optimal position falls at the 80 particles in whatever correlation coefficient or the mean random error. Even though it is improved by increasing the number of image to 8192 pairs, the trend still exists. All data show some fluctuations as compared with the actual flow profile in Figure 4b. Besides, there are no obvious differences in the total errors in Figure 5b. However, we can observe from Figure 6b that the higher densities seem to perform slightly better than the lower. A reasonable interpretation to this is the dense concentration can provide higher probability of particle showing up in the picture, thus increasing the SNR. Noted that it should only work when the maximum displacement is not large such as five pixels in this study. Accordingly, the particle density is expected shifting to lower number as the maximum displacement increases.

3.3 Search Radius

Four search radiuses were considered here, namely 6, 7, 9, and 12 pixels. In Figure 4c and Figure 5c, the results of SR=6 pixels seriously deviate from the normal track. The major differences take place between Y=18 to 46 pixels in Figure 4c and after the actual displacement of four pixels in Figure 5c. Obviously, the discrepancies were resulted from insufficient spatial information included in the computed region. The same trend is also observed in Figure 6c, indicating at least 7 pixels of search radius is required to show the complete displacement in the whole area. After moving over the threshold, the size of the search radius does not influence the results drastically. As concerning the number of image, the results are not improved quite much from the increasing number, either.

3.4 Particle image size

Another interesting factor that might influence the result is the particle image size. Similarly, there were four sizes generated for the simulated particle images without background noise. Based on the past researches (*Westerweel et al., 1997; Prasad et al., 1992*), an optimal value around two to three pixels would result in least variance in conventional PIV. However, here the results seem to behave differently in SPE as shown in Figure 6d. It illustrates that smallest particle, i.e. one pixel, has lower mean random error and higher correlation coefficient than the other particle image sizes. In contrast, six-pixel particle has poor performance and we can expect that the situation will deteriorate as the size keeps increasing. Unfortunately, the small particle image is almost impossible in microscopic world due to the light diffraction limit. Hence, one should always put extra efforts to make the smallest particle image possible if the accuracy is concerned. Similar to particle density, there is not much difference between various particle image sizes with respect to total error (shown in Figure 5d) as well as all of the calculated data show perfect agreement with the actual flow profile in Figure 4d. Meanwhile, compared with the other three factors, the influence coming from particle image size is minor under the current conditions.

3.5 FFT-CC vs. SPE

Additional comparisons were also accomplished between the FFT-CC and SPE for understanding how the SPE could behave under the same SNR. FFT-CC was simulated for one and eight image pairs with and without background noises. The particle density was 40 particles over a 64×64 pixel image. The computations were conducted with an interrogation window size of 32×32 pixels and 50% window overlap. Subsequently, a displacement vector map of 3×3 grids was obtained. The SPE of identical SNR was 1024 and 8192 image pairs with and without background noises. With a search radius of 12 pixels, the vectors at the corresponding positions were selected for comparisons. The results are depicted in Figure 8. For the case without background noise (BG=0 out of 8-bit gray scale intensity index), the SPE has lower measurement errors and excellent coincidence with the actual displacement (Table 1). Especially, the improvement of the error is evident as the number of image increases eight times. For the case with background noise (BG=60), however, the results reverse except for the correlation coefficient (Table 1). FFT-CC behaves relatively stable due to higher SNR from the spatial information over a larger area. Besides, the main reason that FFT-CC deviates from the actual displacement seriously is due to its ambiguous determination of the direction in the strong velocity gradient.

4. Conclusion

A series of simulated particle images with respect to four different factors, namely image quality, particle density, search radius, particle image size, were evaluated. Fixed image size, 64×64 pixels, with a parabolic flow profile of a maximum five-pixel displacement was used through the entire study. Based on the indices of measurement errors and correlation coefficient, the results were discussed in detail. The comparisons indicated that the image quality primarily dominated the accuracy and reliability of SPE among the investigated factors. Oppositely, the particle image size has the least influence to SPE. Under the minimum required SNR, i.e. 1024 image pairs which is identical the condition using 32×32 interrogation window, the optimal value subjected to individual factor was derived from the findings. Regarding the image quality, image SNR higher than 12.39 dB should be reached in order to obtain an acceptable result. Alternatively, improvement was able to be made by increasing the number of image as well. The appropriate particle density was suggested 80 particles over the 64×64 image. Typically, as long as the search radius was over certain number of pixels, the accuracy differences between search radiuses were not obvious. Eventually, the result implied the minimum requirement for the radius was actual displacement plus two to three extra pixels. Furthermore, the findings showed that the best result always tended to the smallest particle image size, i.e. one pixel. Even though it was not attainable in the microscopic world due to the light diffraction limit, one should always try to approach the smallest value. Another interesting comparison between FFT-CC and SPE showed the SPE performed better than FFT-CC over all indices in ideal conditions; however, it got worse when background noise was included. This phenomenon implies more than expected number of image should be used in the real measurement in order to reach the same accuracy in the conventional cross-correlation. As a whole, all the accuracy and reliability except for the bias error could be effectively improved by increasing the number of image.

At present, general criteria from the characterization of SPE had been revealed for the accurate PIV computation. Based on the ideal conditions subjected to the four factors, the total errors would be less than 0.2 pixels as well as the correlation coefficient would almost approach 1. Experimental measurements followed by the rule will be proceeded to verify their feasibility in the near future.

5. Acknowledgement

The authors are grateful to the support from BIRCK Nanotechnology Center at Purdue.

6. References

- Chen J, Katz J (2005) Elimination of peak-locking error in PIV analysis using the correlation mapping method. *Meas. Sci. Technol.* 16:1605–1618.
- Fincham AM, Spedding GR (1997) Low cost, high resolution DPIV for measurement of turbulent fluid flow. *Exp. Fluids* 23:449-462.
- Gui L, Wereley ST (2002) A correlation-based continuous window-shift technique to reduce the peak-locking effect in digital PIV image evaluation. *Exp. Fluids* 32:506–517.
- Huang H, Diabiri D, Gharib M (1997) On the error of digital particle image velocimetry. *Meas. Sci. Technol.* 8:1427–1440.
- Meinhart CD, Wereley ST, Santiago JG (2000) A PIV Algorithm for Estimating Time-Averaged Velocity Fields. *Journal of Fluids Engineering* 122:285-289.

Prasad K, Adrian RJ, Landreth CC, Offutt PW (1992) Effect of resolution on the speed and accuracy of particle image velocimetry interrogation. *Exp. Fluids* 13:105–116.

Sud, A. (2005) Nano-Velocimetry: Single Pixel Evaluation for Particle Image Velocimetry, Thesis, Purdue University.

Wereley ST, Meinhart CD, Gui L, Tretheway D, Sud A (2005) Single Pixel Evaluation of Microchannel Flows. *Proceeding of IMECE2005*, November 5-11, 2005, Orlando, Florida USA.

Westerweel J (1997) Fundamentals of digital particle image velocimetry. *Meas. Sci. Technol.* 8:1379–1392.

Westerweel J, Geelhoed PF, Lindken R (2004) Single-pixel resolution ensemble correlation for μ PIV applications. *Exp. Fluids* 37:375-384.

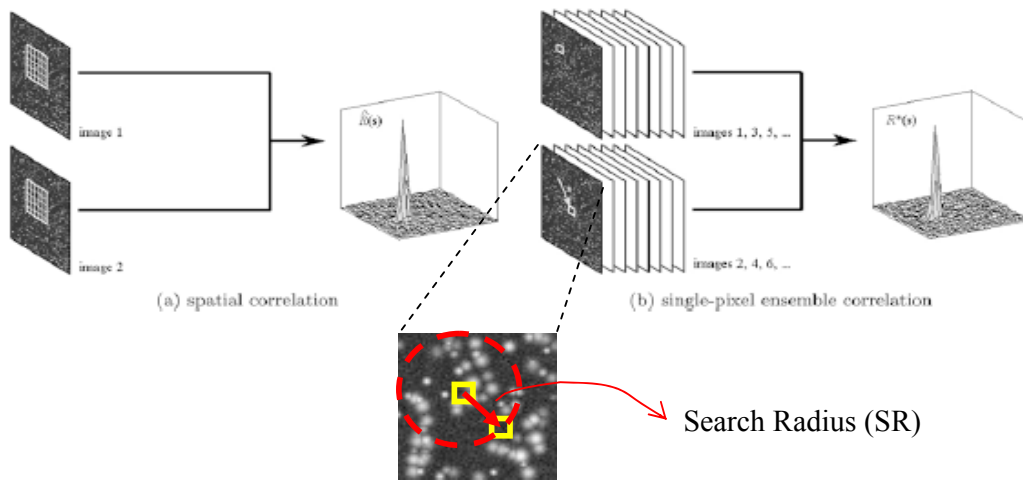


Figure 1 Schematic comparison of (a) spatially-averaged cross correlation algorithm (customary) compared to (b) the Single Pixel Evaluation algorithm (Westerweel, et al., 2004).

Image Quality					
	1.34 dB	2.5 dB	5.58 dB	12.39 dB	47.96 dB
Particle Density					
	20 particles	40 particles	80 particles	160 particles	200 particles
Particle image size					
	1 pixel	2 pixels	4 pixels	6 pixels	6 pixels

Figure 2 Simulated particle images with respect to image quality (first row), particle density (second row), and particle image size (third row).

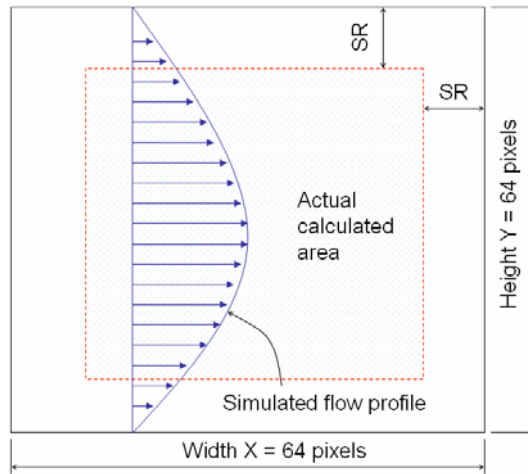


Figure 3 Schematic diagram of the actual evaluated area and the simulated particle image. Four strips associated with the search radius around the bound are excluded during computation. A parabolic curve governs the particle displacement within the image.

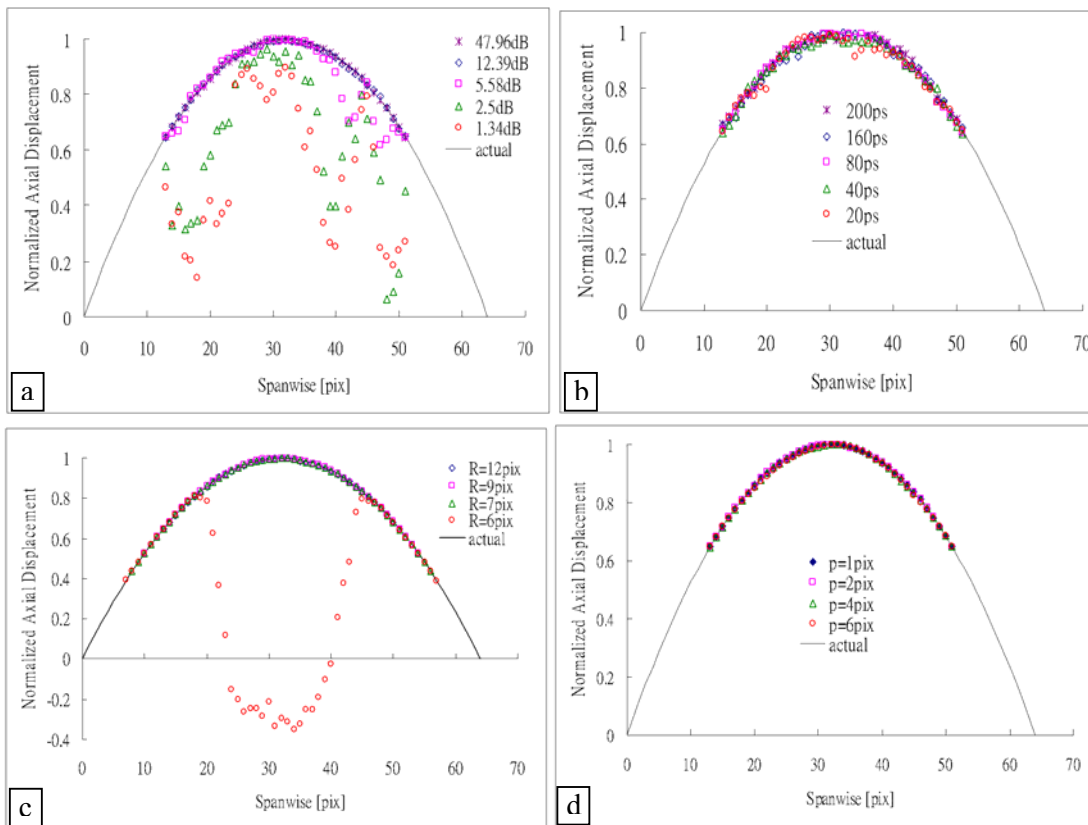


Figure 4 Comparisons of flow profile with 1024 image pairs. The dots are computed data based on difference parameters. The solid line stands for the actual displacement. The factor concerned in each sub-figure is (a) image quality, (b) particle density, (b) search radius, (d) particle image size.

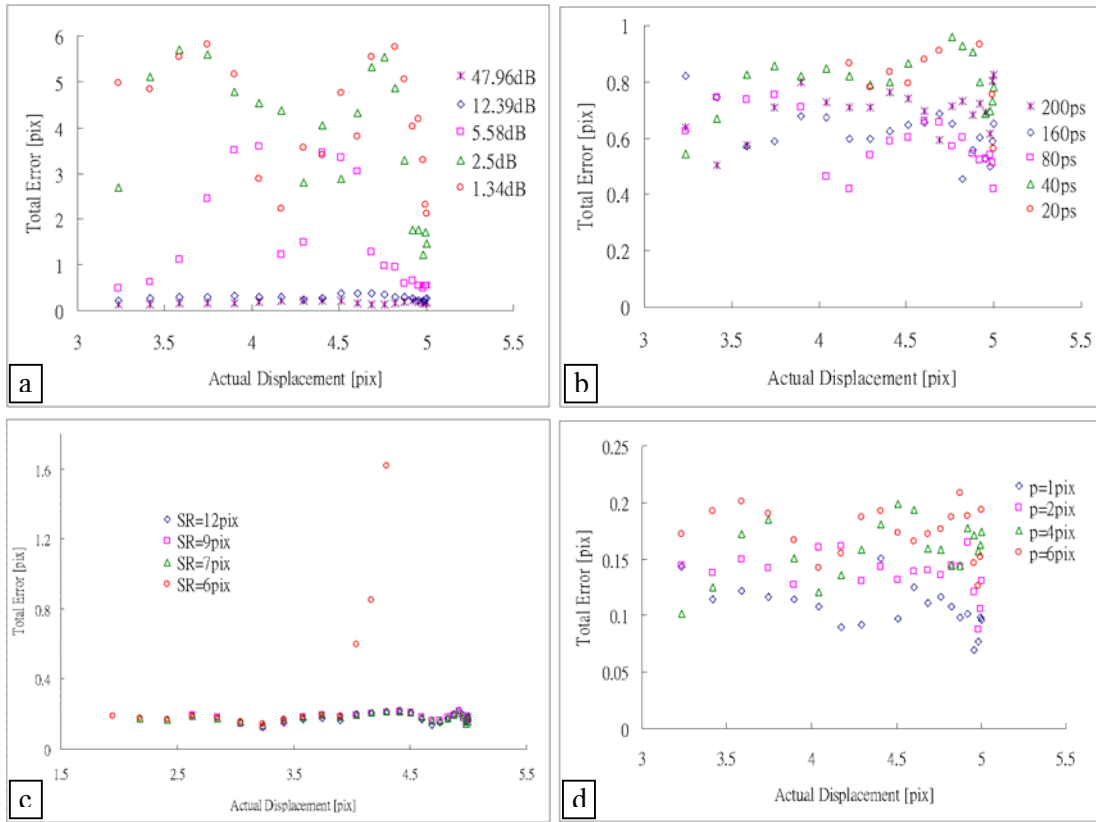


Figure 5 Comparisons of total error (δ) with 1024 image pairs. The factor concerned in each sub-figure is (a) image quality, (b) particle density, (b) search radius, (d) particle image size.

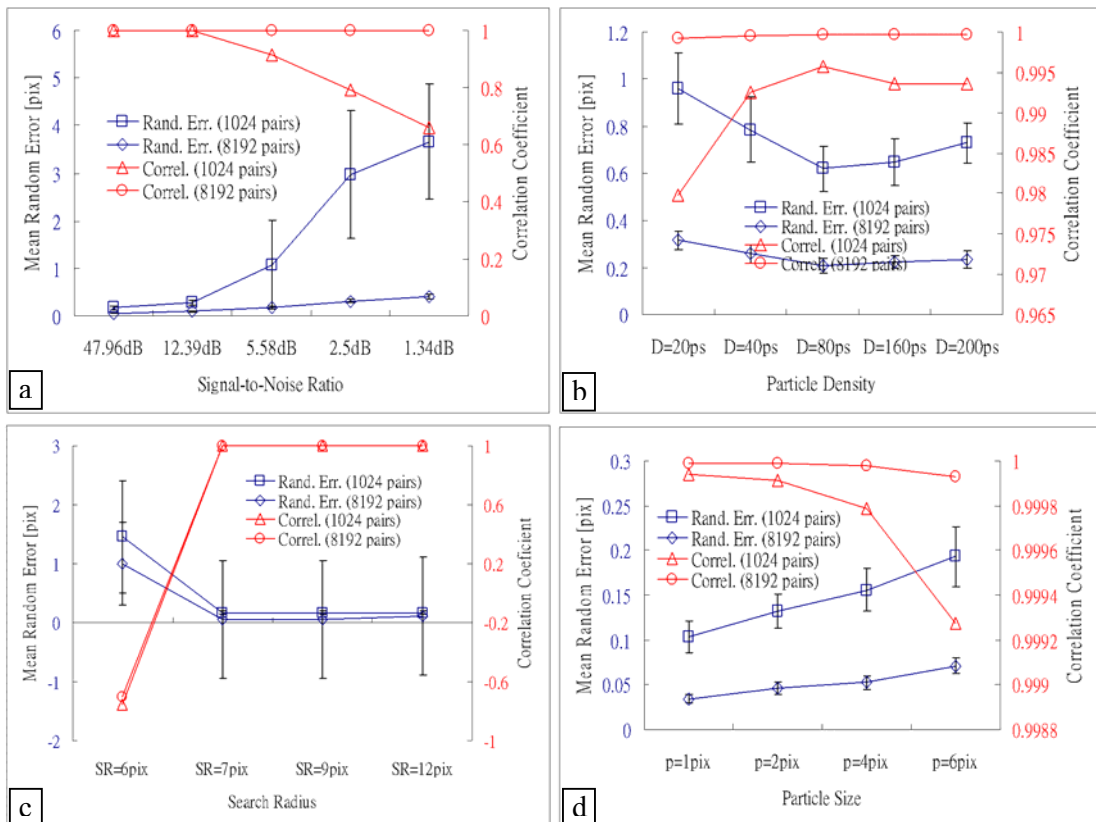


Figure 6 Comparisons of the mean random error (σ) and cross-correlation (R^2). The error bar stands for the variance of the σ . The factor concerned in each sub-figure is (a) image quality, (b) particle density, (b) search radius, (d) particle image size.

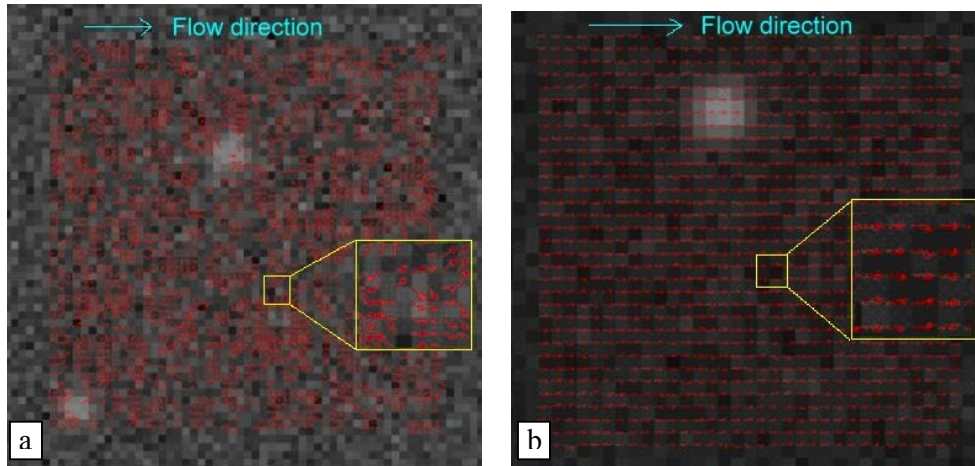


Figure 7 The SPE vector maps of simulated images with different conditions. (a) low density and poor contrast with 2048 image pairs (b) the same conditions after thresholding.

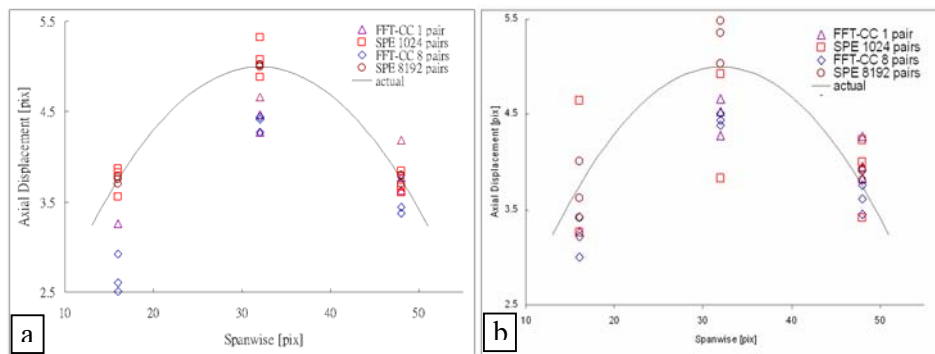


Figure 8 The comparisons of flow profiles between FFT-CC and SPE. (a) BG=No; (b) BG=60

Table 1 FFT-CC vs. SPE

40 particles, SR=12pix, B=130-250, BG=60					40 particles, SR=12pix, B=130-250, BG=No				
	1 pair cc	1024 SPE	8 pairs cc	8192 SPE		1 pair cc	1024 SPE	8 pairs cc	8192 SPE
$\bar{\sigma}$	0.356	0.815	0.142	0.198	$\bar{\sigma}$	0.392	0.171	0.116	0.036
Std.	0.248	0.358	0.076	0.122	Std.	0.263	0.051	0.090	0.021
R^2	0.685	0.946	0.951	0.993	R^2	0.730	0.999	0.907	0.999